BİTLİS EREN ÜNİVERSİTESİ
FEN BİLİMLERİ DERGİSİ

ISSN: 2147-3129 / e-ISSN: 2147-3188

Article Type : Research Article
Received : July 15, 2025
Revised : October 9, 2025
Accepted : October 10, 2025
DOI : 10.17798/bitlisfen.1741940

Year : 2025
Volume : 14
Issue : 4
Pages : 2438-2455

AERODYNAMIC OPTIMIZATION OF THE CESSNA 172 PROPELLER VIA COMPUTATIONAL FLUID DYNAMICS

Mehmet Ali GORDEBIL [1], **Mikail TEMİREL** [1,*]

[1] *Abdullah Gul University, Mechanical Engineering Department, Kayseri, Türkiye*

***Corresponding Author:** mikail.temirel@agu.edu.tr*

ABSTRACT

The term "Light Aircraft" refers to aircraft weighing less than 5.5 tons. The term light aircraft refers to aircraft weighing less than 5.5 tons. These aircraft formed the backbone of air forces during both world wars, primarily powered by propellers, and continue to be widely used today for flight training, travel, recreation, and personal use. Cessna, a leading light aircraft manufacturer, introduced the Cessna 172 in 1956—a model that remains in production. However, its limited speed and altitude performance fall short of modern aviation requirements. To address these limitations, a computational fluid dynamics (CFD) study was conducted using Ansys Fluent and CFX to enhance the aircraft's aerodynamic efficiency and speed. Design modifications were applied to the propeller, with a focus on improving thrust generation. The modified configuration produced a significant improvement: CFD results indicated an approximately 50% increase in thrust, corresponding to a 21% increase in the maximum velocity of the aircraft. This study highlights the potential of CFD tools to optimize classic aircraft designs such as the Cessna 172, providing practical insights for the modernization of light aircraft in both civilian and military applications.

Keywords: Design of propeller, Speed of aircraft, Cessna 172, Computational fluid dynamics (CFD).

1 INTRODUCTION

The term "Light-Weight Aircraft" refers to single-engine, low-cost-to-produce aircraft that weigh less than 5.5 tons, or approximately 12,000 pounds[1]. These aircrafts can commonly be found in service as personal property as well as being the backbone in fighter pilot and aviator training, whether it is for military or commercial purposes. Cessna was one of the

License: CC BY-NC 4.0

leading manufacturers of these aircrafts until the company ceased. Various models of these aircraft are still in use, specifically in military training. It is crucial to note that maintenance squads commonly apply handmade improvements to these aircraft, as they have the potential to deliver more, thanks to their robust airframe[2]. The reason for this is Cessna's common design philosophy, which emphasizes the production of structurally reliable machinery. The Cessna 172 is one of these models, featuring a robust chassis design capable of handling speeds up to 500 km/h at a peak altitude of over 15,000 feet. However, the design currently achieves only 300 km/h at an altitude of 13,000 feet[3]. The Cessna 172 is an improvement of the base model 170, and it remains in active production by the parent company, Textron, as it continues to receive a substantial amount of interest[3]. It is also easy to implement basic improvements on the aircraft to increase its performance in terms of higher altitude, speed, and fuel efficiency. However, as of now, there is no professional attempt to implement improvements supported by engineering studies. One of the significant parameters affecting the altitude and speed limitations of these models is the design of the propeller, which can be viewed as a rotating wing composed of multiple airfoils, similar to the cross-section of an aircraft wing.

In propeller-driven airplanes, the propeller plays a crucial role in generating both lift and forward thrust, enabling take-off, altitude gain, and mid-flight acceleration by converting the rotational energy from the engine shaft. The cambered shape of the airfoil causes the airflow in front of the blade to accelerate, contributing to this forward motion. Propellers generate lift in two ways: through horizontal displacement like a wing using airfoil design, and by producing thrust when rotating at high speeds. When the aircraft pitches up, the angle of attack on the downward-moving blade becomes greater than the upward-moving blade, generating additional lift that pushes the nose upward. The physical rule behind it can be explained by Bernoulli’s principle[4, 5], which states that the acceleration of airflow in front of the propeller reduces static pressure, while the slower airflow behind it results in higher static pressure. This pressure difference pulls the aircraft forward due to the reaction force. The thrust generated by this pressure difference enables the aircraft to overcome drag and maintain forward motion. In summary, the propeller design significantly affects the lift and thrust to reach maximum lift and thrust to minimize the aircraft’s altitude and speed limitations.

To increase the performance of the propeller, there are mainly two ways, including experimental and numerical studies in the literature. Typically, an experimental study of a propeller is conducted in a wind tunnel under controlled conditions[6, 7]. For example, Brandt et al.[8] carried out an experimental study in a wind tunnel to evaluate the performance of 79

small-scale propeller blades operating at low Reynolds numbers. Deters et al.[9] applied a similar method using a different type of propeller blade. They tested the performance of 27 small-scale propellers, collecting data on thrust, power, and efficiency across a specific range of advance ratios. In another study, the aeroacoustic features of propellers were analyzed at the small unmanned aerial vehicles (UAV)[10]. Yilmaz et al.[11] conducted an experimental study to analyze the performance characteristics and velocity field of a 16-inch diameter ducted propeller using five different duct shapes at zero angle of attack. The power coefficients for all ducted propeller configurations were found to be lower than those of an open propeller, indicating that propellers operate more efficiently when enclosed within a duct. Experimental studies often yield the most accurate results, but they are costly and time-consuming. To minimize the cost of experimental studies and to estimate results early, computational analysis has become increasingly popular in the field.

The second method of propeller analysis is Computational Fluid Dynamics (CFD) studies, which is a specialized branch of fluid dynamics widely applied across various engineering disciplines. It combines numerical analysis and computational software to tackle complex fluid-related challenges[12]. The significance of CFD is particularly evident in aerospace engineering, where it enables the precise analysis of fluid flow under various boundary conditions, helping engineers identify and address potential design flaws early in the development process[13]. This makes CFD a valuable tool in the research and development (R&D) sectors of industries[14]. Its applications extend beyond aerospace and automotive engineering, finding increasing use in the aviation sector as researchers explore its practical benefits[15]. Additionally, CFD is recognized as a cost-effective solution that delivers highly accurate results, often comparable to experimental findings[16-18].

Within the scope of propeller design, CFD has been a crucial tool for testing specified design parameters, such as velocity, shear stress, and pressure, as well as calculating lift and thrust. Testing these parameters with multiple repetitions increases both the cost and the time required to obtain accurate results. CFD reduces the number of repetitions, thereby making it more efficient for research[15]. For instance, Kutty et al. performed a CFD study to analyze the small APC slow flyer propeller blade via Ansys Fluent and validated it with available experimental data[19]. Their results demonstrated reliable data for thrust coefficient, power coefficient, and efficiency in scenarios with low advance ratios, as well as for advance ratios below the negative thrust conditions. In a study, a commercial AG-Nel 25 aircraft was modified with the conceptual design methods via CFD to be used in agricultural applications. They

optimized the wings, fuselage, and pilot ergonomics as well as its propeller[20]. In another study, a CFD method was employed to address the issues of inadequate thrust and high drag values in the high-altitude long-endurance unmanned aerial vehicle (HALE UAV)[21]. CFD studies on propellers have been applied not only in aviation technology but also in marine vehicles[22]. For example, Broglia et al. conducted a study to investigate the impact of propeller modeling on predicting the dynamic behavior of a manoeuvring vessel[23]. For this purpose, the turning circle manoeuvre of a twin-screw ship with a single rudder was thoroughly analyzed using the RANS solver χ-navis in combination with various propeller models. In a similar study, ship maneuverability modeling was analyzed using CFD body force, propeller, and free-running simulations[24].

In this study, certain design improvements were made by applying the principles of advanced engineering, specifically Fluid Dynamics, to the Cessna 172 aircraft. The design improvements were conducted by investigating the propeller. We redraw the existing model of the propeller in SolidWorks and conducted the computational analysis. According to their results, designs were modified to improve the performance of aircraft. Then, similar analyses were performed under the same conditions to demonstrate the superiority of the new designs. The propeller blades can be adjusted accordingly to yield higher performance to prevent “bottle-necking”. Overall, this paper provides an understanding of how to approach light aircraft design by enhancing the performance of a very popular model.

2 METHODOLOGY

2.1 Propeller Design

The sizes and dimensions of the original designs of the Cessna 172 propeller were obtained from the literature[25]. The propeller was then modeled in SolidWorks based on the provided scales, with a scale ratio of 1:14, to improve mesh quality and reduce simulation time. The propeller blades were analyzed in three separate sections: the base, middle, and edge, as shown in Figure 1a. The technical drawings of these three parts are shown in Figure 1b, highlighting their corresponding positions. The three parts were then modified by adjusting the chord length, height, and angles, as depicted in Figure 1c. Adjustments were made to ensure that the air is compressed effectively, creating a low-pressure area and increasing the velocity of the air flowing through it. This is achieved in accordance with Bernoulli’s principle, where a "low-pressure area" is generated by reducing the distance between the surface of the airfoil

and the upper layers of airflow. The sizes of the designs were labeled with letters, and all dimensions for the designs are provided in Table 1.

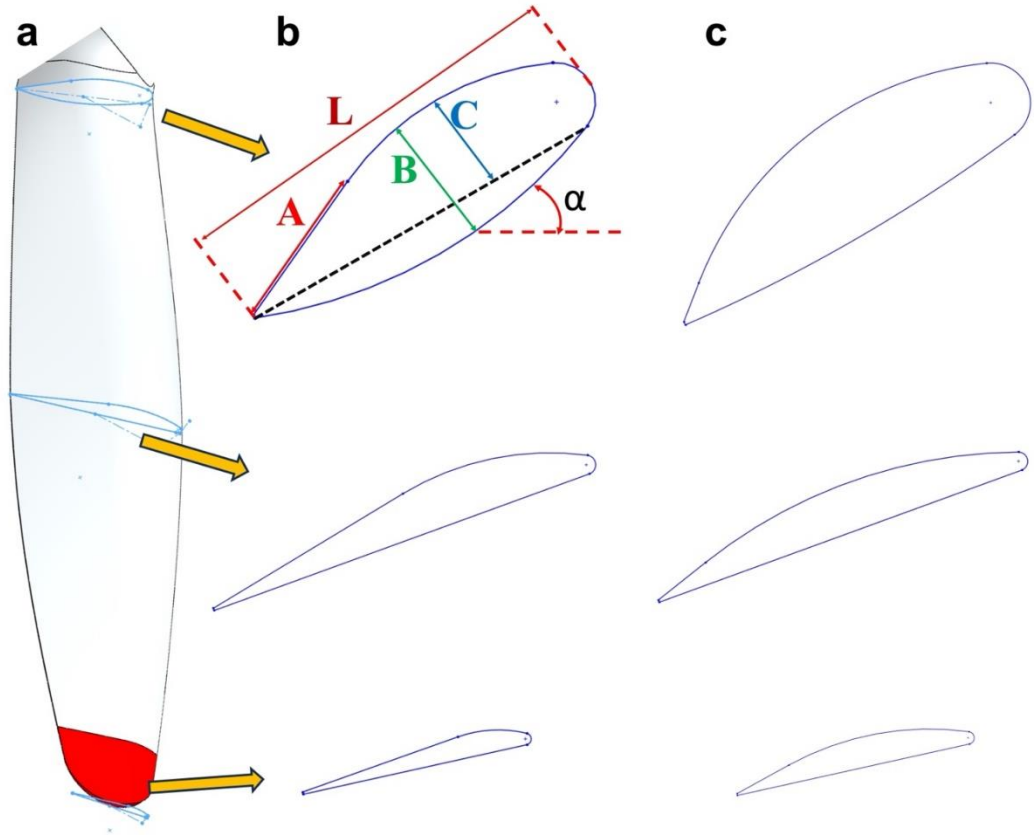


Figure 1. Propeller design illustrating airfoil variations along the blade: (a) CAD drawing of one side of the original Cessna 172 propeller, (b) three sections of the original airfoil, including the base, middle, and edge, where dimensions at the base are indicated with capital letters to highlight design modifications, and (c) the modified design. Scale Ratio is 1:14.

Table 1. Real and adjusted values of the propeller blade at a scale ratio of 1:14.

	A (mm)	B (mm)	C (mm)
Base	50	40	30
Base – Adjusted	12.6	35	32
Middle	92	21	-
Middle – Adjusted	26	20.55	-
Edge	56	8	0.8
Edge – Adjusted	20	10	0.6

2.2 Simulation Setting

This section highlights the essential aspects of the CFD analysis conducted for the fluid flow around the propeller. It covers critical stages of the process, including assumptions, mesh generation, boundary condition definition, and simulation configuration.

2.2.1 Assumptions & Simulation Setup

Assumptions for the simulation were made to closely resemble real-world conditions. Required values for air at altitudes above 12,000 ft were taken from thermodynamic tables[26] as presented in Table 2. The relationship between lift-to-weight ratio and altitude gain was assumed to be linear for calculating the maximum altitude gain, even though it behaves exponentially beyond a certain point, as experimentally determined for each aircraft model by NASA. A steady flow was assumed, with no heat transfer occurring between the friction surface of the propeller and the surrounding airflow. The material used in the model was selected as aluminum, consistent with its actual material. The system analyzed is an open adiabatic system, where only mass flows through it. As the temperatures of the airflow and solid remain constant and identical, there is no heat transfer between the wall and the fluid, resulting in zero heat flux.

Table 2. Air properties at 12,000 ft and chosen air speed[5, 26].

Property	Values
Density ($\frac{kg}{m^3}$)	0.653
Inlet velocity ($\frac{m}{s}$)	83.889
Characteristic length of propeller (m)	0.068
Viscosity ($Pa \cdot s$)	1.592×10^{-5}
Atmospheric pressure (atm)	0.56

The viscosity models in Ansys Fluent are highly dependent on the fluid's flow characteristics under the specified conditions. To address this, the Reynolds number was first calculated using the following equation: Re= ρvl/μ, where v, ρ, l, and μ represent velocity (m/s), fluid density (kg/m³), characteristic length (m), and viscosity (Pa·s), respectively. According to Cengel and Cimbala, flows with a Reynolds number greater than 5×10^5 are classified as turbulent[5]. As the calculated Reynolds numbers for all flows across the various characteristic

lengths of both propeller geometries are considerably above 5×10^5, it can be concluded that the flow throughout the airfoil is turbulent.

In the simulation, the two-equation standard k-ε viscosity model was selected due to the subsonic turbulent flow of propeller geometries. Residual monitors were set as 0.0001 for continuity, x-velocity, y-velocity, z-velocity, k, and ε equations.

2.2.2 Mesh Generation

Meshing involves dividing the object's regions into small cells through which fluid particles will move. The solver software subsequently applies the relevant equations to each cell during the next steps. Before initiating meshing, it is essential to define and label the required surfaces and flow regions (Figure 2a). Once these regions are labeled, the meshing process is carried out. An average element size of 0.0001 meters in the propeller over 0.22 meters, resulting in more than 1.5 million elements for the propeller, as seen in Figure 2c. The coefficient of y+ value for NACA 2412 is approximated as 1 through the upper boundary layer to get highly precise results.

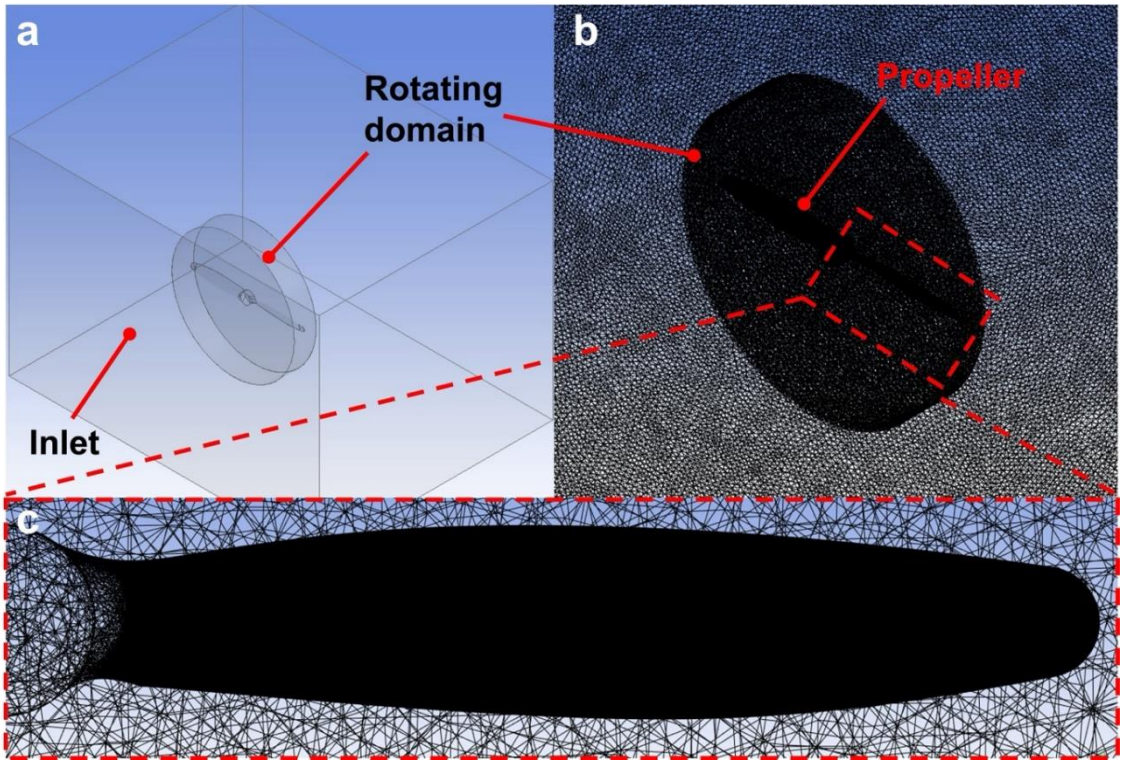


Figure 2. Flow and rotation domains, along with the meshes of the propeller. (a) Flow domain showing the inlet and rotating domain for the propeller. (b) Mesh for the rotating domain, including the propeller blade. (c) Detailed view of the propeller blade.

Moreover, a mesh independence analysis was conducted by evaluating maximum velocity and maximum pressure as the number of mesh elements increased. Two figures were plotted to illustrate the fluctuations in the results with varying mesh densities, as seen in Figure 3. Significant changes were observed up to approximately 600,000 mesh elements. Beyond this point, the results began to stabilize and fluctuations were minimized, indicating mesh independence.

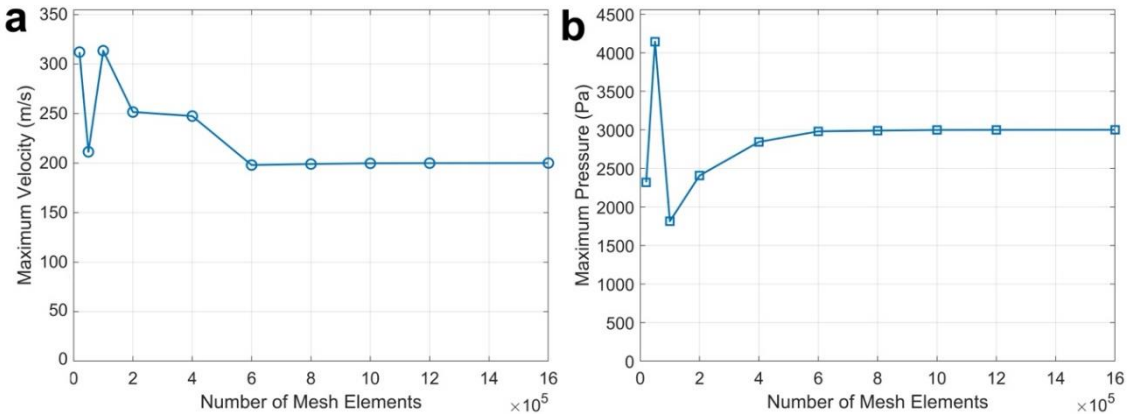


Figure 3. Mesh independence analysis for varying numbers of elements, ranging from 0 to 1.6 million. a) Changes in maximum velocity. b) Changes in maximum pressure.

2.2.3 Boundary Condition

Establishing appropriate boundary conditions is crucial, as the simulation relies on the conditions under which the system is defined. These conditions must closely mimic real-world properties to ensure meaningful and accurate results. In this study, it is important to highlight that the same boundary conditions were applied to both the original designs of the Cessna 172's propeller and the improved designs proposed for the propeller. This approach ensured the results were directly comparable. To define the boundary conditions, a rectangular enclosure was first established to serve as a control volume, encompassing the propeller, depending on the simulation (Figure 2a). In the Fluent simulations, the surroundings were defined as walls, with an inlet and outlet specified at the front and back. For the CFX simulations, the surroundings were modeled as openings, and an additional cylindrical enclosure was created around the propeller to simulate the rotating domain. The inlet velocity was set at 83.8889 m/s, as provided by the company, representing the optimal cruising velocity during a significant portion of the flight. Finally, in the CFX simulations, the angular velocity within the rotating domain was defined as 2700 RPM, corresponding to the operating speed at which the Continental O-300 engine reaches the "red line."

3 RESULTS

3.1 Fluent Results of Propeller

The solution converged after 109 iterations out of 1000 for the specified viscosity model and residuals. As mentioned in the design section, the propeller blade design incorporates three different airfoils. Therefore, the simulation was performed at the transition points where the blade geometry changes to a new airfoil. Specifically, three planes were assigned to these transition points, and three contours were defined on them. These contours provided the velocity profile and pressure distribution profile along the blade surface. For clarity, the planes were positioned at $x = 0.11$, $x = -0.015$, and $x = -0.065$, based on the length of the enclosure. These positions correspond to the locations of the airfoils along the blade. The simulation was conducted for the blade, and the resulting velocity profiles and pressure distributions are shown in Figures 4 and 5, respectively, for both the original and improved propeller blade geometries.

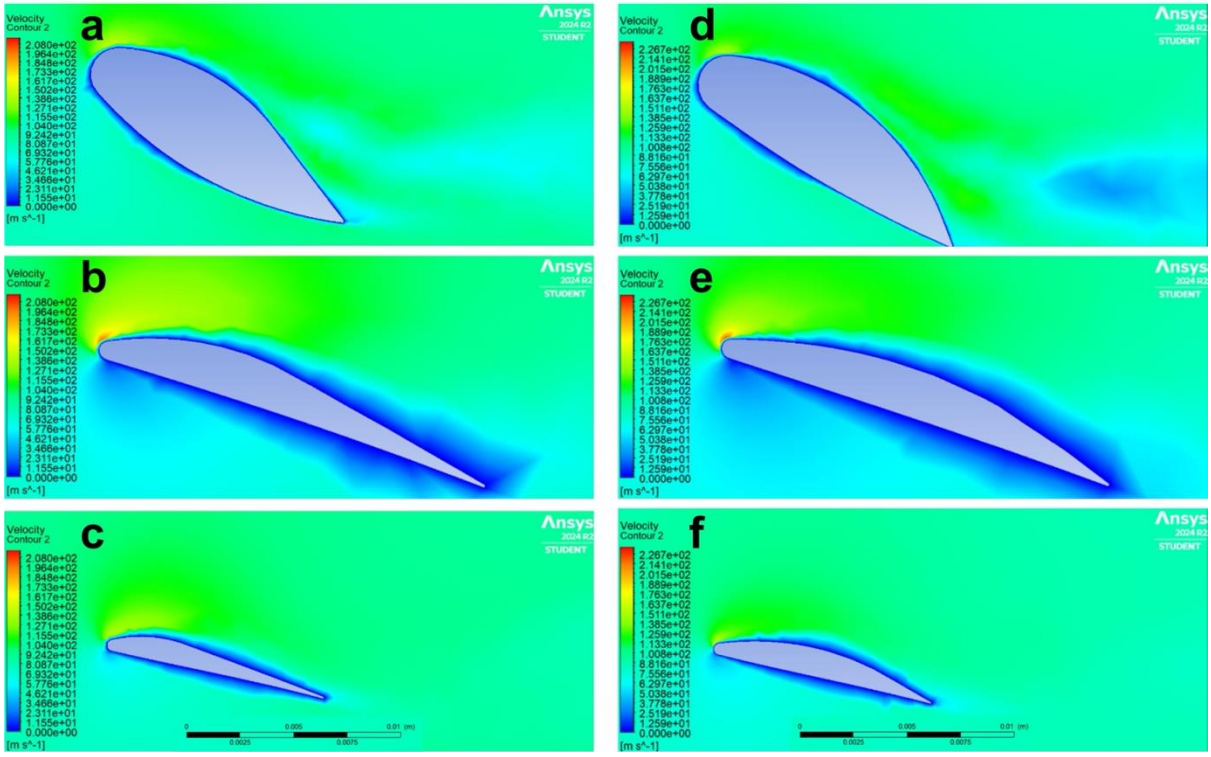


Figure 4. Fluent velocity contour results for (a) base, (b) middle, and (c) edge airfoils along the original blade, and (d) base, (e) middle, and (f) edge airfoils along the improved blade.

In Figure 4, the results for the original design are displayed in the left column, while the results for the improved design are shown in the right column. Particular attention should be given to the wake in the velocity field behind the airfoil, especially for the original design. This

wake, caused by flow separation, generates turbulence, which reduces the thrust produced by the propeller and significantly impacts its performance by increasing drag[27]. It is evident, particularly in the middle comparison between the existing and improved designs (Figures 4b and 4e), that the wake behind the original design is larger than that of the improved design. This reduction in wake due to the design modification leads to increased thrust and improved fuel efficiency.

Lift primarily occurs due to the pressure differences between the lower and upper surfaces of the airfoil, which can be explained using Bernoulli's principle. In this context, the difference in contour colors between the original and improved designs on the lower and upper surfaces of the airfoils, particularly in the middle section (see Figures 5b and 5e), indicates an increased pressure difference in the improved model, as shown in Figure 5. This significant increase in pressure difference generates a substantial amount of lift in the middle section of the propeller blade, effectively enhancing its ability to push upward[28].

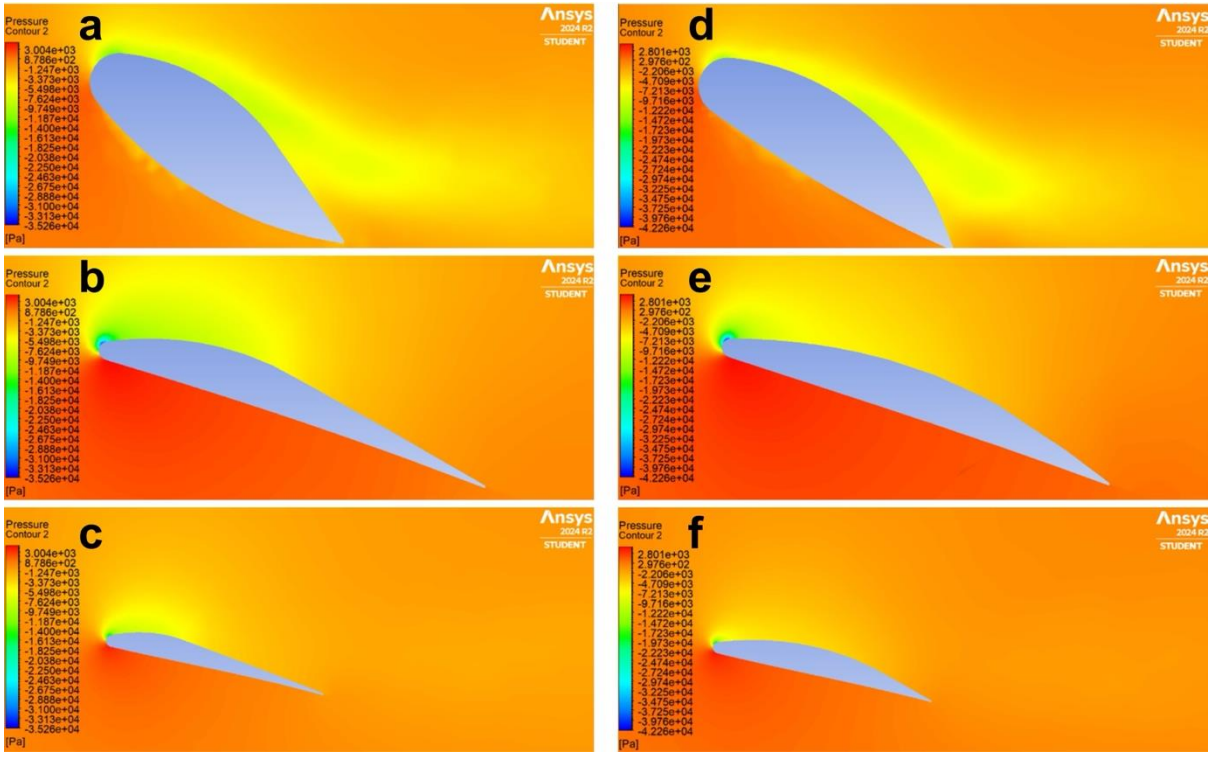


Figure 5. Fluent pressure contour results for a) base, b) middle, and c) edge airfoils along the original blade, and d) base, e) middle, and f) edge airfoils along the improved blade.

To quantitatively demonstrate the improvement in the design, rather than relying solely on visual inspection of the contours, we calculated the drag and thrust forces based on both literature data and CFD results. The drag force D[29]:

$$D = C_d * \rho * \frac{V^2}{2} * A \quad (1)$$

Where C_d is the drag coefficient, ρ is the air density at the given altitude, V is the air velocity, and A is the frontal area of the wing. The drag coefficient of the scale model Cessna 172 was taken as 0.64[25], while the air density was assumed to be 0.653 kg/m³, as listed in Table 2. The inlet velocity was approximated as 83.889 m/s. The frontal area was estimated by accounting for the fuselage width and height, as well as protruding parts, resulting in an approximate value of 1.11 m² for both models. Since the design adjustment did not significantly alter the frontal area of the propeller, this value was used for the calculations. Based on the equation, the drag force was calculated to be 3.26 kN.

This drag value, obtained for the scaled model, was subsequently used to calculate the thrust-to-drag ratios for both the adjusted and the baseline models. The following calculations present the thrust force generated by the scaled model of the original propeller design[5].

$$\vec{F} = m_{body}a = \sum_{in} \beta \dot{m} \vec{V} - \sum_{out} \beta \dot{m} \vec{V} \quad (2)$$

Where $\dot{m}$ is the mass flow rate that is equal to the density times the volume flow rate. Then, the volume flow rate is also equal to velocity times area. When we substitute these in equation 2, the thrust force will be:

$$F = \rho * V_{set} * A * (V_{inlet} - V_{otlet}) \quad (3)$$

The velocity V_{set} was predefined in the simulations as 83.8889 m/s. The inlet and outlet air velocities were obtained from the contour plots using a probe in Ansys, as shown in Figure 4. The inlet flow velocities (V_{inlet}) were measured as approximately 105 m/s and 115 m/s for the actual and adjusted designs, respectively, while the outlet velocity was nearly identical for both models at around 84 m/s. This value is very close to the free-stream velocity, further confirming the validity of the simulation setup.

Based on Equation (3), the thrust forces were calculated as 19.2 kN for the actual design and 28.31 kN for the adjusted design, corresponding to nearly a 50% increase in thrust with the new configuration at the given altitude. Regarding the thrust/drag ratio for the actual and adjusted designs, they are around 5.889 and 8.68, respectively. A staggering 47.37% increase in thrust/drag ratio. Through the relation between speed and thrust/drag ratio, speed is a function

of the square root of thrust/drag ratio. But we approximated the equal inlet air velocity, and the drag was calculated the same for both designs. In this case, the effect of drag is eliminated. Then, the relationship between thrust (T) and velocity (Equation 4), expressed as $T \propto V^2$, the increase in the aircraft's maximum speed at the specified altitude can be determined. This relationship allows the effect of the thrust enhancement on overall aircraft performance to be quantified;

$$\frac{V_2}{V_1} = \sqrt{\frac{T2}{T1}} \tag{4}$$

Where T represents thrust. Accordingly, the velocity ratio between the actual and adjusted designs was calculated as 1.213, corresponding to a 21.3% increase in speed due to the design modifications. This improvement indicates that the adjusted configuration is more aerodynamically efficient, capable of achieving a greater range with the same fuel capacity, while imposing less stress on the engine and ensuring more stable performance at cruising altitude.

These findings indicate that the adjusted design generates a greater thrust force for the propeller during horizontal motion. However, as noted earlier, because the propeller operates as a rotating machine, this type of simulation alone is insufficient to draw definitive conclusions. Therefore, it is necessary to further analyze the results obtained from the CFX simulations of the improved propeller design.

3.2 CFX Results for Propeller

Out of 1000 iterations, convergence for the CFX solution, considering the specified viscosity model and residuals, was achieved at the 44th outer loop iteration. The subsequent section presents the results of the propeller's CFX simulation. As previously discussed, the CFX simulation is particularly effective for analyzing rotating (turbo) machinery. Hence, it is unnecessary to evaluate the blade components individually, as the entire propeller can be simulated as a unit. The results, including velocity and pressure contours, are illustrated in Figures 6 and 7, respectively.

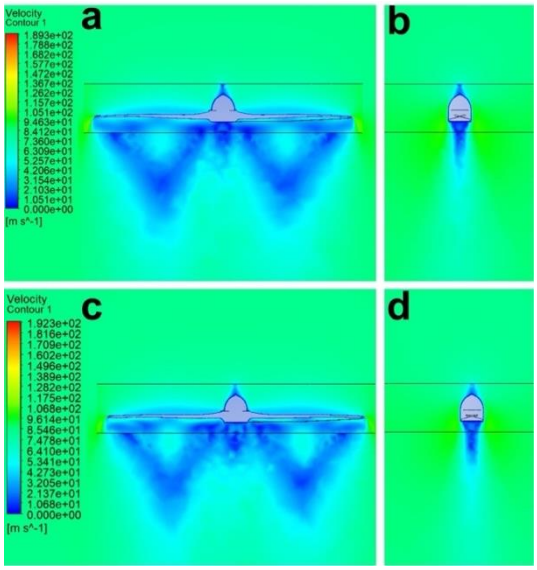


Figure 6. CFX velocity contour results for (a, b) the original propeller and (c, d) the improved propeller.

It might initially seem confusing when observing the figures that the high-pressure zone appears at the front. However, it should be noted that this represents the air pressure when it encounters the propeller, rather than the overall pressure distribution (Figure 7). To further clarify this, the y-x plane (side view) has also been included on the right side. As can be clearly observed from the figure, the leading edge of the propeller creates a vortex effect on the exiting air. Additionally, in the pressure contour, the impact of the stagnation point is distinctly visible. Despite this, the rotating propeller successfully accelerates the air, as evident in the pressure contour, where it generates a high-pressure field at the rear and a low-pressure field at the front. This pressure difference is what produces thrust force. Enhancing the magnitude of the pressure difference between these zones will result in increased thrust generation[30].

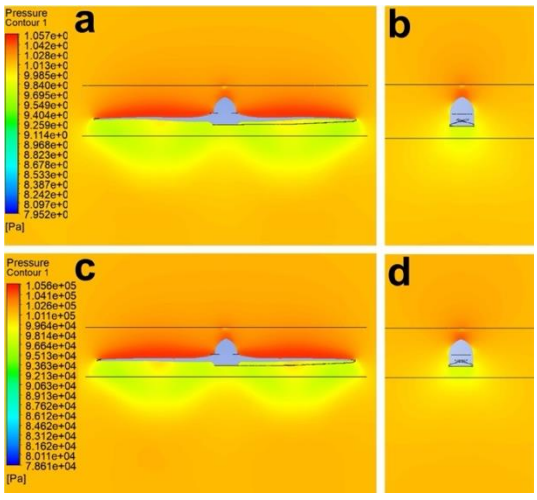


Figure 7. CFX pressure contour results for (a, b) the original propeller and (c, d) the improved propeller.

In the improved model, the air vortex generated at the leading edge of the previous propeller is significantly reduced. When comparing the figures, it is evident that the improved propeller (Figures 7c and 7d) produces a greater pressure difference, resulting in higher thrust force and achieving higher velocity readings (Figures 6c and 6d). Additionally, the y-z planes, which provide a clearer depiction of the uniform velocity contours behind the propeller, further confirm the superiority of the adjusted design.

The primary strength of CFX software lies in its ability to analyze streamlines rather than contours. Figure 8 illustrates the streamlines defined at the opening and around the propeller for both the original and improved designs. Upon examining the figures, it becomes evident that the Cessna 172's original propeller design lacks sophistication in effectively distributing air (Figure 8a). This results in the generation of a large vortex, which disrupts the airflow velocity and diminishes the pressure difference between the front and back of the propeller. Consequently, this reduces the thrust force that the propeller can generate[30]. Additionally, the figure illustrates that the original propeller disperses the streamlines, causing wake air to form behind and around the aircraft. This wake air increases drag, reduces velocity, and negatively impacts fuel efficiency[31]. However, this issue is not present in the improved design, as the updated propeller produces a more refined and well-organized streamline profile (Figure 8c). Notice how the air does not accumulate around the propeller but is instead pushed outward due to the propeller rapidly increasing the velocity of the incoming air and dispersing it. This action subsequently propels the surrounding air outward, as illustrated by the streamlines in Figure 8c. This demonstrates the enhanced thrust force generated by the improved propeller, as the surrounding air also moves faster compared to the original design.

From the comparisons in Figure 8b and 8d, it is evident that the new model not only moves through the air at a faster rate but also promotes laminar flow, reducing turbulence compared to the original design (Figure 8b). Unlike the random separation points observed in the original design, the proposed design (Figure 8d) ensures a more predictable and uniform separation pattern. This improvement increases thrust, minimizes turbulence around the propeller and aircraft body, reduces drag, enhances fuel efficiency, and ultimately increases the aircraft's maximum velocity[32].

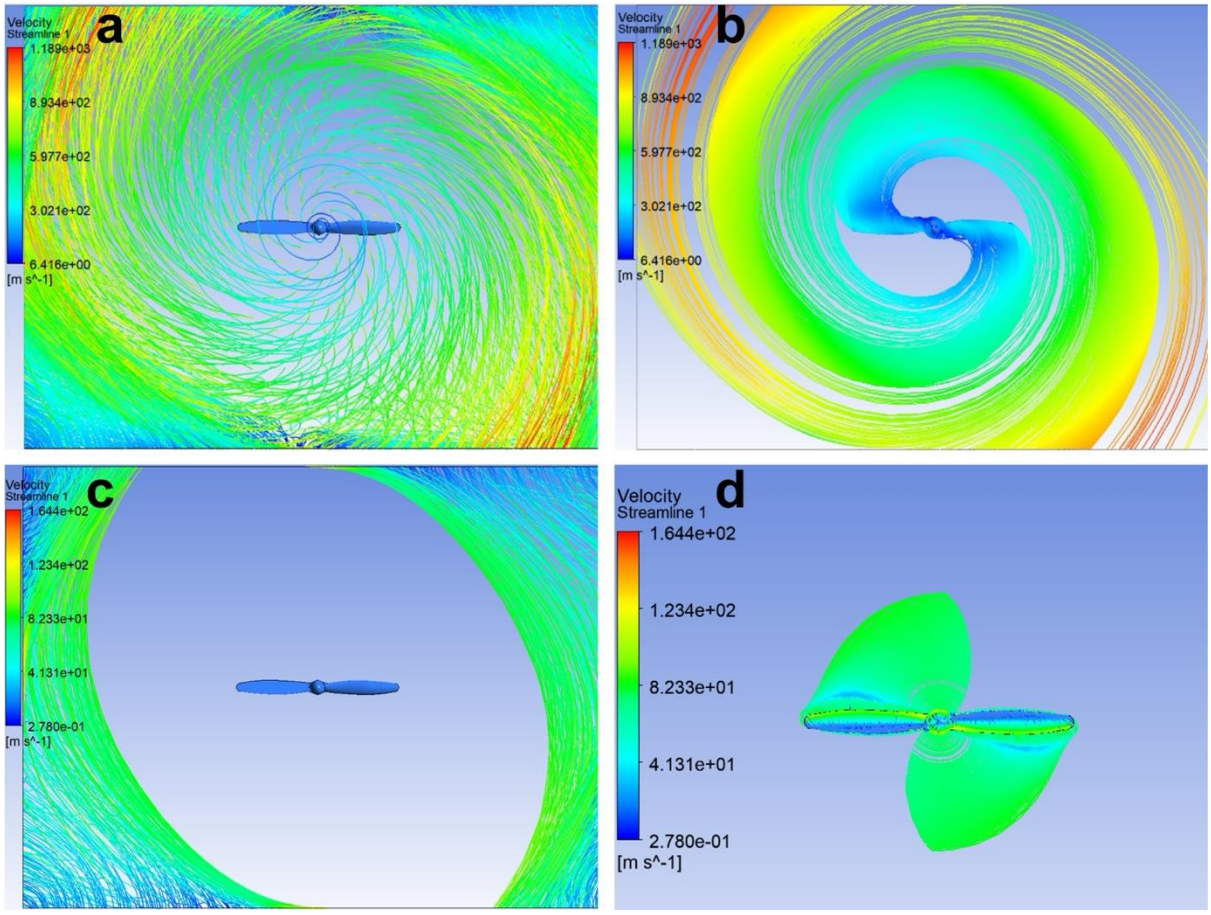


Figure 8. CFX streamlines are defined at the openings for a) the original design and c) the improved design, and at the propeller for b) the original design and d) the improved design.

4 CONCLUSION

In conclusion, an in-depth analysis of the project's findings has been conducted. Upon examining these results, it is evident that the project's initial aims have been successfully achieved. To address the limitations of the Cessna 172, such as its inability to achieve high velocity and altitude, we conducted CFD studies to improve the original propeller designs. The propeller blades were analyzed in three separate sections—base, middle, and tip—for both the original and modified designs. The study demonstrated that even minor design modifications can enhance the maximum velocity by around 21% and the overall efficiency of the aircraft. Additionally, the new propeller design improved thrust by around 50% and fuel efficiency by generating higher pressure differences between the upper and lower surfaces of the airfoil compared to the original design.

This study not only highlights the robustness of the Cessna 172's airframe and its capacity to withstand more than its original design intended, but also provides a guideline for future research on integrating advanced aerodynamic applications into legacy aircraft. Although

conducted on a lightweight aircraft, this study can be extended to various models and serve as a steppingstone for future research on the application of CFD in aerodynamic studies.

Conflicts of Interest

There is no conflict of interest between the authors.

Author Contributions

Conceptualization, M.T.; methodology, visualization, formal analysis, M.T. and M.A.G.; validation, data curation, writing—original draft preparation, M.T. and M.A.G.; writing—review and editing, M.T.; project administration, supervision, M.T. All authors have read and agreed to the published version of the manuscript.

Acknowledgments

The authors would like to acknowledge Abdullah Gul University for giving them the opportunity to work together.

REFERENCES

[1] D. Crane, "Dictionary of aeronautical terms," *(No Title),* 1997.

[2] R. Smith, *Cessna 172: a pocket history*. Amberley Publishing Limited, 2010.

[3] H. BASAK and A. Akdemir, "Design Optimization of Cessna 172 Wing With Biomimetic Design Approach," (in en), *https://ijpte.com/index.php/ijpte,* Research Article 2024-06-26 2024, doi: https://ijpte.com/index.php/ijpte/article/view/66.

[4] M. T. Sultan, O. J. Lee, J. S. Lee, and C. H. Park, "Three-Dimensional Digital Light-Processing Bioprinting Using Silk Fibroin-Based Bio-Ink: Recent Advancements in Biomedical Applications," *Biomedicines,* vol. 10, no. 12, Dec 12 2022, doi: 10.3390/biomedicines10123224.

[5] Y. Cengel and J. Cimbala, *Ebook: Fluid mechanics fundamentals and applications (si units)*. McGraw Hill, 2013.

[6] Z. Tang, P. Liu, Y. Chen, and H. Guo, "Experimental Study of Counter-Rotating Propellers for High-Altitude Airships," *Journal of Propulsion and Power,* vol. 31, no. 5, pp. 1491-1496, 2015, doi: 10.2514/1.B35746.

[7] Z. Ning and H. Hu, "An Experimental Study on the Aerodynamic and Aeroacoustic Performances of a Bio-Inspired UAV Propeller," presented at the 35th AIAA Applied Aerodynamics Conference, 2017.

[8] J. Brandt and M. Selig, "Propeller performance data at low reynolds numbers," 2011, p. 1255.

[9] R. W. Deters, G. K. Ananda Krishnan, and M. S. Selig, "Reynolds Number Effects on the Performance of Small-Scale Propellers," presented at the 32nd AIAA Applied Aerodynamics Conference, 2014.

[10] G. Sinibaldi and L. Marino, "Experimental analysis on the noise of propellers for small UAV," *Applied Acoustics,* vol. 74, no. 1, pp. 79-88, 2013, doi: 10.1016/j.apacoust.2012.06.011.

[11] S. Yilmaz, D. Erdem, and M. S. Kavsaoglu, "Performance of a ducted propeller designed for UAV applications at zero angle of attack flight: An experimental study," *Aerospace Science and Technology,* vol. 45, pp. 376-386, 2015, doi: 10.1016/j.ast.2015.06.005.

[12] E. I. Basri, A. A. Basri, V. N. Riazuddin, S. F. Shahwir, Z. Mohammad, and K. A. Ahmad, "Computational fluid dynamics study in biomedical applications: a review," *International Journal of Fluids and Heat Transfer,* vol. 1, no. 2, pp. 2-14, 2016.

[13] P. R. Spalart and V. Venkatakrishnan, "On the role and challenges of CFD in the aerospace industry," *The Aeronautical Journal,* vol. 120, no. 1223, pp. 209-232, 2016.

[14] R. Hajili and M. Temirel, "Computational Fluid Dynamics (CFD) Analysis of 3D Printer Nozzle Designs," *Bitlis Eren Üniversitesi Fen Bilimleri Dergisi,* vol. 13, no. 4, pp. 1233-1246, 2024.

[15] A. Rizzi and J. M. Luckring, "Historical development and use of CFD for separated flow simulations relevant to military aircraft," *Aerospace Science and Technology,* vol. 117, 2021, doi: 10.1016/j.ast.2021.106940.

[16] O. J. Boelens, "CFD analysis of the flow around the X-31 aircraft at high angle of attack," *Aerospace Science and Technology,* vol. 20, no. 1, pp. 38-51, 2012.

[17] M. N. U. Fareez, A. A. S. Naqvi, M. Mahmud, and M. Temirel, "Computational Fluid Dynamics (CFD) Analysis of Bioprinting," *Advanced Healthcare Materials,* 2024, doi: 10.1002/adhm.202400643.

[18] M. Temirel, B. Yenilmez, S. Knowlton, J. Walker, A. Joshi, and S. Tasoglu, "Three-Dimensional-Printed Carnivorous Plant with Snap Trap," *3D Printing and Additive Manufacturing,* vol. 3, no. 4, pp. 244-251, 2016, doi: 10.1089/3dp.2016.0036.

[19] H. Kutty and P. Rajendran, "3D CFD Simulation and Experimental Validation of Small APC Slow Flyer Propeller Blade," *Aerospace,* vol. 4, no. 1, 2017, doi: 10.3390/aerospace4010010.

[20] P. D. Bravo-Mosquera, H. D. Cerón-Muñoz, G. Díaz-Vázquez, and F. Martini Catalano, "Conceptual design and CFD analysis of a new prototype of agricultural aircraft," *Aerospace Science and Technology,* vol. 80, pp. 156-176, 2018/09/01/ 2018, doi: https://doi.org/10.1016/j.ast.2018.07.014.

[21] F. A. Maulana, E. Amalia, and M. A. Moelyadi, "Computational fluid dynamics (CFD) based propeller design improvement for high altitude long endurance (HALE) UAV," *International journal of intelligent unmanned systems,* vol. 11, no. 3, pp. 425-438, 2023.

[22] K.-W. Kim, K.-J. Paik, J.-H. Lee, S.-S. Song, M. Atlar, and Y. K. Demirel, "A study on the efficient numerical analysis for the prediction of full-scale propeller performance using CFD," *Ocean Engineering,* vol. 240, p. 109931, 2021/11/15/ 2021, doi: https://doi.org/10.1016/j.oceaneng.2021.109931.

[23] G. D. Riccardo Broglia , Danilo Durante Andrea Di Mascio, "Simulation of turning circle by CFD: Analysis of different propeller models and their effect on manoeuvring prediction," vol. 39, ed: Applied Ocean Research, 2013.

[24] S. Li, C. Liu, X. Chu, M. Zheng, Z. Wang, and J. Kan, "Ship maneuverability modeling and numerical prediction using CFD with body force propeller," *Ocean Engineering,* vol. 264, 2022, doi: 10.1016/j.oceaneng.2022.112454.

[25] C.-w. Kim and S. L. O. California Polytechnic State University, "Scale modeling of Cessna 172," California Polytechnic State University, San Luis Obispo, 2011. [Online]. Available: https://digitalcommons.calpoly.edu/cgi/viewcontent.cgi?article=1041&context=aerosp[Online]. Available: https://digitalcommons.calpoly.edu/aerosp/36

[26] Y. A. Cengel, "Thermodynamics: an engineering approach," ed: McGraw-Hill, 2011.

[27] W. Zhang, W. Cheng, W. Gao, A. Qamar, and R. Samtaney, "Geometrical effects on the airfoil flow separation and transition," *Computers & Fluids,* vol. 116, pp. 60-73, 2015, doi: 10.1016/j.compfluid.2015.04.014.

[28] M. D. Patterson and N. K. Borer, "Approach considerations in aircraft with high-lift propeller systems," 2017, p. 3782.

[29] *Drag Force and Drag Coefficient | 3 | v2 | Aircraft Performance | Moha*. 2025.

[30] R. Gill and R. D. Andrea, "Propeller thrust and drag in forward flight," in *2017 IEEE Conference on Control Technology and Applications (CCTA)*, 27-30 Aug. 2017 2017, pp. 73-79, doi: 10.1109/CCTA.2017.8062443.

[31] K. Biber, "Estimating propeller slipstream drag on airplane performance," *Journal of Aircraft,* vol. 48, no. 6, pp. 2172-2174, 2011.

[32] A. Filippone, *Advanced aircraft flight performance*. Cambridge University Press, 2012.